

Wavefront Reconstruction from Noisy Fringe Observations via Sparse Coding

Vladimir Katkovnik¹, José Bioucas-Dias², Hongxing Hao^{3,2}

¹Department of Signal Processing, Technology University of Tampere

²Instituto de Telecomunicações, Instituto Superior Técnico, TULisbon,
1049-001 Lisboa, Portugal. E-mail: bioucas@lx.it.pt

³College of Information Systems and Management, National University of Defense
Technology, Changsha, Hunan, China. E-mail: hongxinghao87@gmail.com

1 Introduction

In this paper, we use sparse modeling for processing phase-shifting interferometry measurements. The proposed approach takes into full consideration the Poissonian (photon counting) measurements. In this way we are targeting at optimal sparse reconstruction both phase and magnitude taking into consideration all details of the observation formation. Many images (and signals) admit sparse representations in the sense that they are well approximated by linear combinations of a small number of functions taken from a known set. The topic of sparse and redundant representations has attracted tremendous interest from the research community in the last ten years. This interest stems from the role that the low dimensional models play in many signal and image areas such as compression, restoration, classification, and design of priors and regularizers, just to name a few [1].

Let $\mathbf{c} \in \mathbb{R}^n$ denote a vector representing an image, or a patch of it, and let us assume that \mathbf{c} admits a *sparse* representation or *sparse coding* with respect to the columns of a given matrix $\Psi \in \mathbb{R}^{n \times m}$; i.e., it is possible to write $\mathbf{c} = \Psi\theta$, where $\theta \in \mathbb{R}^m$ is a vector containing only a few non-zero components. The matrix Ψ is termed a synthesis operator (or dictionary) because in the writing $\mathbf{c} = \Psi\theta = \sum_{j=1}^m \Psi_j \cdot \theta_j$, where Ψ_j are the columns of Ψ and θ_j are the elements of θ , \mathbf{c} is synthesized as a linear combination of the columns of Ψ weighted by the elements of θ , often called the *spectrum* of \mathbf{c} . The synthesis based representations have a dual point of view in which, given an image $\mathbf{a} \in \mathbb{R}^n$, we compute its spectrum $\beta \in \mathbb{R}^m$ by applying the so-called analysis operator (or dictionary) $\Phi \in \mathbb{R}^{m \times n}$ to \mathbf{a} , i.e., $\beta = \Phi\mathbf{a}$. It happens that when we are looking

for the sparsest approximation using a synthesis dictionary, the likelihood of success increases with the number and variety of signals (atoms) hold by the dictionary. As a consequence, the synthesis dictionaries yielding sparse representations are often *overcomplete*, i.e., $m < n$. The concept of *frame* is a generalization of the classical basis especially developed for overcomplete (synthesis and analysis) representations with linearly dependent approximating functions [1].

Let $\mathbf{o} \in \mathbb{C}^m$ be a complex valued wavefront defined on a grid with m pixels. Denote $\mathbf{B}_o = \text{mag}(\mathbf{o})$ and $\varphi_o = \text{angle}(\mathbf{o})$ as, respectively, the corresponding images of magnitude and phase. Then we have $\mathbf{o} = \mathbf{B}_o \exp(j\varphi_o)$. Herein, all functions applied to vectors are to be understood in the component-wise sense; the same applies to multiplications and divisions of vectors.

In sparse coding for complex valued images we may think in two different approaches: either we use a complex valued sparse representation to model directly the complex image \mathbf{o} , as recently proposed in [2], or we use sparse real valued representations for the magnitude and absolute phase images of \mathbf{o} [3]. In this paper we follow the second approach mentioned above. It gives:

$$\text{mod}(\mathbf{o}) = \Psi_a \theta_{a,o}, \quad \text{angle}(\mathbf{o}) = \Psi_\varphi \theta_{\varphi,o}, \quad (1)$$

$$\theta_{a,o} = \Phi_a \cdot \text{mod}(\mathbf{o}), \quad \theta_{\varphi,o} = \Phi_\varphi \cdot \text{angle}(\mathbf{o}), \quad (2)$$

where $\theta_{a,o}$ and $\theta_{\varphi,o}$ are, respectively, the magnitude and the phase spectra of the object \mathbf{o} . Eqs. (1) synthesize the magnitude ($\text{mod}(\mathbf{o})$) and phase ($\text{angle}(\mathbf{o})$) from the magnitude and phase spectra $\theta_{a,o}$ and $\theta_{\varphi,o}$. On the other hand, the analysis Eqs. (2) give the spectra for magnitude and phase of the wavefront \mathbf{o} .

2 Phase-shifting interferometry

For the L -step phase-shifting interferometry the complex-valued wave field at the sensor plane is given by

$$\mathbf{u}_s = \mathbf{B}_o \exp(j\varphi_o) + \mathbf{A}_r \exp(-j\varphi_r) \in \mathbb{C}^N, \quad s = 1, \dots, L, \quad (3)$$

where $\mathbf{B}_o \exp(j\varphi_o)$ and $\mathbf{A}_r \exp(-j\varphi_r)$ are the object and reference fields respectively. Let us assume that our sensor takes measures on a rectangular grid

with N digital elements and let $\mathbf{Y}_s = \{\mathbf{Y}_s[l], l=1, \dots, N\}$ for $s=1, \dots, L$ denote the L measured images with N elements each. The measurement process in optics amounts to count the photons hitting the sensor's elements and is well modeled by independent Poisson random variables; that is

$$P(\mathbf{Y}_s[l] = k) = \exp(-\mathbf{I}_s[l]\chi) \frac{(\mathbf{I}_s[l]\chi)^k}{k!}, \quad k = 0, 1, \dots, \quad (4)$$

where k is an integer number of photons, \mathbf{I}_s is the intensity $\mathbf{I}_s = |\mathbf{u}_s|^2$, thus given by

$$\mathbf{I}_s = \mathbf{B}_o^2 + \mathbf{A}_r^2 + 2\mathbf{B}_o\mathbf{A}_r \cos(\varphi_o + \varphi_{r_s}), \quad s = 1, \dots, L, \quad (5)$$

and χ is a scaling parameter of the Poissonian flow which can be interpreted as an exposure time (and/or as a sensitivity of the sensor). We recall that the mean and the variance of $\mathbf{Y}[l]$ are equal and given by $\mathbf{I}_s[l]\chi$.

3 Wavefront reconstruction

In this paper, we consider the problem of wavefront reconstruction as estimation of $\mathbf{o} = \mathbf{B}_o \exp(j\varphi_o)$ from observations $\mathbf{Y}_s = \{\mathbf{Y}_s[l], l=1, \dots, N; s=1, \dots, L\}$ assuming that \mathbf{A}_r and φ_{r_s} are given. In our experiments φ_{r_s} takes values $0, \pi/2, \pi, 3\pi/2$. Herein, we adopt a multiobjective optimization approach [3] to find an object $\mathbf{o} = \mathbf{B}_o \exp(j \cdot \varphi_o)$ which satisfies

$$\mathbf{u} = \arg \min_{\mathbf{u}} L_1(\mathbf{u}, \mathbf{v}), \quad (\mathbf{B}_o, \varphi_o) = \arg \min_{\mathbf{B}_o, \varphi_o} L_2(\mathbf{B}_o, \varphi_o, \mathbf{u}), \quad (6)$$

$$(\theta_{B_o}, \theta_{\varphi_o}) = \arg \min_{\theta_{B_o}, \theta_{\varphi_o}} L_3(\theta_{B_o}, \theta_{\varphi_o}, \mathbf{B}_o, \varphi_o), \quad (7)$$

$$\text{s.t.} \quad \mathbf{v}_s = (\Psi_a \theta_{B_o}) \exp(\Psi_\varphi \theta_{\varphi_o}) + \mathbf{A}_r \exp(-j\varphi_{r_s}), \quad s = 1, \dots, L, \quad (8)$$

where

$$\begin{aligned} \mathbf{L}_1(\mathbf{u}, \mathbf{v}) &= \sum_{s=1}^L \sum_{l=1}^N [|\mathbf{u}_s[l]|^2 \chi - \mathbf{Y}_s[l] \log(|\mathbf{u}_s[l]|^2 \chi) + \\ &\frac{1}{\gamma_1} \sum_{s=1}^L \|\mathbf{u}_s - \mathbf{v}_s\|_2^2, \end{aligned} \quad (9)$$

$$\mathbf{L}_2(\mathbf{B}_o, \varphi_o, \mathbf{u}) = \sum_{s=1}^L \|\mathbf{u}_s - (\mathbf{B}_o \exp(j\varphi_o) + \mathbf{A}_r \exp(-j\varphi_r))\|_2^2, \quad (10)$$

$$\mathbf{L}_3(\theta_{B_o}, \theta_{\varphi_o}, \mathbf{B}_o, \varphi_o) = \tau_a \cdot \|\theta_{B_o}\|_0 + \frac{1}{2} \|\theta_{B_o} - \Phi_{B_o} \mathbf{B}_o\|_2^2 + \quad (11)$$

$$\tau_\varphi \cdot \|\theta_{\varphi_o}\|_0 + \frac{1}{2} \|\theta_{\varphi_o} - \Phi_{\varphi_o} \varphi_o\|_2^2, \quad (12)$$

with $\mathbf{u} = \{\mathbf{u}_s, s=1, \dots, L\}$ and $\mathbf{v} = \{\mathbf{v}_s, s=1, \dots, L\}$. Here the l_0 norm of θ , denoted as $\|\theta\|_0$, counts the number of non-zero elements of θ and promotes the sparsity of approximation for phase and magnitude.

The variable \mathbf{v} in (9) corresponds to a quadratic splitting introduced to decompose the likelihood term in two more manageable objective functions \mathbf{L}_1 and \mathbf{L}_2 . The indices B_o and φ_o in the frames stress the fact these frames are adapted to the signals they represent. We conclude therefore that the multiobjective optimization (6)-(7) aims at finding objects which are simultaneously likely to have produced the observation \mathbf{Y}_s and have sparse representations.

The developed iterative algorithm (**S**parse **P**hase **A**mplitude **R**econstruction (**SPAR**)) is based on alternating solution of the problems (6)-(7). In our implementation of SPAR we adopt the flexible BM3D-frames (**B**lock-**M**atching and **3D** filtering) for sparse approximation of absolute phase and magnitude [3] and for the phase unwrapping the state-of-the-art PUMA algorithm [4], which is able to cope with piecewise smoothed phase surfaces.

The SPAR algorithm is initialized with \mathbf{v}_s^0 . Provided that we are given \mathbf{A}_r , then an estimate for \mathbf{B}_o and φ_o can be obtained by minimizing $\sum_{s=1}^L \|\mathbf{Y}_s - (\mathbf{B}_o^2 + \mathbf{A}_r^2 + 2\mathbf{B}_o \mathbf{A}_r \cos(\varphi_o + \varphi_r))\|_2^2$, yielding the solution which is well known for processing of phase-shifting interferometry data:

$$\tan(\varphi_o^\dagger) = \frac{\mathbf{Y}_4 - \mathbf{Y}_2}{\mathbf{Y}_1 - \mathbf{Y}_3}, \quad \mathbf{B}_o^\dagger = \sqrt{\sum_{s=1}^4 (\mathbf{Y}_s - \mathbf{A}_r^2)/4}. \quad (13)$$

However, these estimates can be very noisy and should be filtered. In our experiments, we use BM3D filtering to initialize the algorithm by \mathbf{B}_o^0 . For filtering of the wrapped phase φ_o^\dagger , we use the PEARLS algorithm [5] obtaining $\varphi_o^0 = \text{PEARLS}(\varphi_o^\dagger)$.

4 Experiments

The interferometric phase in PEARLS is estimated based on the first order local polynomial approximation with a varying adaptive neighborhood. We are focused on SPAR phase reconstructions and on comparing these results with those of PEARLS. Recall that, because PEARLS is derived based on the simple exponential observation model $\mathbf{u}_s = \exp(j\varphi_o) + \mathbf{w}$, where \mathbf{w} is Gaussian noise, the estimates provided by this algorithm are not optimal. On the other hand, SPAR is derived considering a much more complex observation model which includes Poissonian noise and measurements of intensities from various phase shifts. Here, a relevant aspect to address is to what extent the increased complexity of SPAR produced better results than PEARLS.

First of all, note that a *good* initialization is needed for SPAR: *good* means that the wrapped phase $\varphi_o^0 = \text{PEARLS}(\varphi_o^\dagger)$ should allow an useful unwrapping by the PUMA algorithm. If this condition is fulfilled, then SPAR is always able to improve the results given by PEARLS. Moreover, the performance of SPAR depends on the parameters of the algorithm $\gamma_1, \tau_a, \tau_\varphi$. These parameters should be tuned in to yield optimal results. In what follows, the quality of the wrapped phase reconstruction is characterized in dB by the improvement in the signal-to-noise-ratio (ISNR) defined as $ISNR = 10 \log_{10} \frac{\|\exp(j\varphi_o^0) - \exp(j\varphi)\|_2^2}{\|\exp(j\varphi_o^{100}) - \exp(j\varphi)\|_2^2}$, where the noisy estimate φ_o^0 is the output of PEARLS, φ is the true phase and φ_o^{100} is SPAR the estimate after 100 iterations.

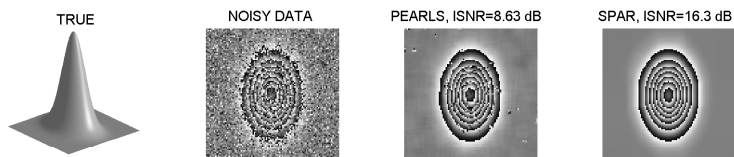


Fig. 1. Left to right: true Gaussian shaped absolute phase; raw noisy phase data, $\sigma=0.89$, phase filtered by PEARLS, SPAR phase reconstruction.

The experiments presented in this section are obtained for a quadratic magnitude \mathbf{B}_o and two examples of the phase surfaces exploited in [5]. Figure 1 and Figure 2 illustrate the visual and numerical advantage of the proposed SPAR algorithm versus the PEARLS algorithm. These results are obtained for very noisy data. For the Gaussian shaped phase in Figure 1 Poissonian observations of the intensities \mathbf{I}_s with the parameter $\chi = 0.15$ yield as the mean value $SNR = 4.8$ dB for each pixel of the sensor. In another terms, the level of this noise can be characterized by the mean number of photons per pixel in each observations. For the considered modeling it is about 9 photon/pixel. Many of random observations take zero value. Figure 2 shows reconstruction of the shear phase plane surface. These results are also given for very noisy data with the parameter $\chi = 0.4$ what yields in average $SNR = 8.56$ dB or 51.3 photon/pixel.

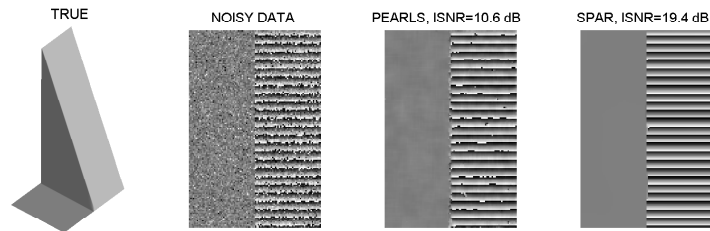


Fig. 2. Left to right: true absolute shear phase plane; raw noisy phase data, $\sigma=0.62$, phase filtered by PEARLS, SPAR phase reconstruction.

5 Conclusion

The variational maximum likelihood technique is developed for phase and magnitude reconstruction of the coherent wavefront from Poissonian intensity measurements in the phase-shifting optical setup. Sparse modeling of magnitude and absolute phase of the wavefront is one of the key elements of the developed algorithm. The experiments show that the new algorithm enables the state-of-the-art accuracy for reconstruction both phase and magnitude of the object wavefront.

6 Acknowledgments

This work is supported by the Academy of Finland, project no. 138207, 2011-2014, and by Fundação para a Ciência e Tecnologia (FCT), Portuguese Ministry of Science and Higher Education, project.PEst-OE/EEI/0008/2013.

7 References

1. M. Elad (2010) *Sparse and Redundant Representations: from Theory to Applications in Signal and Image Processing*, Springer.
2. H. Hongxing, J. M. Bioucas-Dias, and V. Katkovnik (2013) Interferometric phase Image estimation via sparse coding in the complex domain. *IEEE Transactions on Geoscience and Remote Sensing*, submitted.
3. V. Katkovnik and J. Astola (2012) High-accuracy wavefield reconstruction: decoupled inverse imaging with sparse modeling of phase and amplitude. *J. Opt. Soc. Am. A* 29 (1), 44 – 54.
4. J. M. Bioucas-Dias and G. Valadão (2007) Phase unwrapping via graph cuts. *IEEE Transactions on Image Processing* 16 (3) 698–709.
5. J. Bioucas-Dias, V. Katkovnik, J. Astola, and K. Egiazarian (2008) Absolute phase estimation: adaptive local denoising and global unwrapping. *Appl. Opt.*, 47(29) 5358–5369.